ENVIRONMENTAL STUDIES

Congo Basin forest loss dominated by increasing smallholder clearing

Alexandra Tyukavina[1]*, Matthew C. Hansen[1], Peter Potapov[1], Diana Parker[1], Chima Okpa[1], Stephen V. Stehman[2], Indrani Kommareddy[1], Svetlana Turubanova[1]

A regional assessment of forest disturbance dynamics from 2000 to 2014 was performed for the Congo Basin countries using time-series satellite data. Area of forest loss was estimated and disaggregated by predisturbance forest type and direct disturbance driver. An estimated 84% of forest disturbance area in the region is due to small-scale, nonmechanized forest clearing for agriculture. Annual rates of small-scale clearing for agriculture in primary forests and woodlands doubled between 2000 and 2014, mirroring increasing population growth. Smallholder clearing in the Democratic Republic of the Congo alone accounted for nearly two-thirds of total forest loss in the basin. Selective logging is the second most significant disturbance driver, contributing roughly 10% of regional gross forest disturbance area and more than 60% of disturbance area in Gabon. Forest loss due to agro-industrial clearing along the Gulf of Guinea coast more than doubled in the last half of the study period. Maintaining natural forest cover in the Congo Basin into the future will be challenged by an expected fivefold population growth by 2100 and allocation of industrial timber harvesting and large-scale agricultural development inside remaining old-growth forests.

INTRODUCTION

The Congo Basin is home to the second largest massif of humid tropical forests (HTFs) after the Amazon, performing globally important ecosystem services and providing livelihood to the regional population (1). The critical role of the Congo Basin rainforests in climate regulation and biodiversity conservation is recognized internationally and has led to establishing collaborative sustainable forest resource management initiatives such as the Central Africa Regional Program for the Environment and the Regional Programme for the Conservation and Rational Use of Forestry Ecosystems in Central Africa. Understanding forest disturbance dynamics in the region as a whole and on the national scale is essential for policy-making and land use planning.

The presented study is focused on the six Congo Basin tropical rainforest countries, namely, Cameroon (CAM), the Central African Republic (CAR), the Democratic Republic of the Congo (DRC), Equatorial Guinea (EQG), Gabon (GAB), and the Republic of the Congo (RoC). Differences in forest disturbance dynamics and drivers among the Congo Basin countries vary owing to geographic, economic, and demographic conditions (table S1); development history; and current policy and institutional factors (2, 3). Historically, forest loss in the Congo Basin has been strongly linked to rural populations and subsistence agriculture (4, 5). However, per-capita food production and food availability vary between Congo Basin countries (Table 1). CAM stands out as a country with improving food production and, in the regional context, relatively strong export and import sectors. The oil-exporting countries GAB, EQG, and RoC form a group of countries exhibiting decreasing food production. High food import levels for RoC and especially GAB reflect the use of oil earnings to support domestic food consumption. Oil exports account for 40 to 50% of the gross domestic product (GDP) in GAB and RoC and 80% of the GDP in EQG. Such high dependence on oil exports has implications for economic and political stability in the face of price shocks, such as those of 2014 to 2016 (6).

CAR has the lowest human development index of all countries (table S1), reflected in Table 1 by marginal food exports and imports, and the highest per-capita food aid shipments in the region. DRC is unique in its declining food production, low food exports and imports, and lack of food aid shipments. DRC is of particular importance, as it is home to 60% of the remaining Congo Basin humid tropical rainforest (7). DRC is also unique because of its population pressure and recent history of conflict and insecurity. The only country similar to DRC in terms of persistent conflict, insecurity, and statelessness is the CAR (table S1). However, DRC dwarfs CAR in terms of total population and HTF resources. With more than 70 million people, DRC is more than twice the population of CAM, CAR, EQG, GAB, and RoC combined (table S1). For the citizens of DRC, which, along with CAR, has a human development index in the bottom 10% of all countries, there are few livelihood options. The vast majority of the population consists of smallholder farmers, who feed not only themselves but also nearby towns and cities (3, 8).

Given the different economic, political, and social contexts within Congo Basin rainforest countries, we can expect within-region variations in land cover and land use change. For example, mineral and petroleum exports tend to discourage deforestation, as oil wealth enables food importation and reduced domestic agricultural output, with GAB a clear example (9). Low populations also help to ensure low rates of disturbance outside of commercial logging operations for countries like GAB, RoC, and EQG (10). Recent investments in agro-industrial development, mainly palm oil, are a relatively new threat to primary forests in the Congo Basin (11). The Tropical Forest Alliance (12), which seeks to implement sustainable palm oil development in Africa, includes CAR, DRC, and RoC as signatories, but not CAM, EQG, or GAB. The Gulf of Guinea countries have logistical advantages in this sector over interior Congo Basin countries, mainly due to proximity to ports. In GAB, the creation of special economic zones around ports is part of new and ambitious development plans that include palm oil expansion (13). Land use and land cover change in low-population, forest resource–rich Congo Basin countries is likely attributable to extractive industries such as logging or agro-industrial development, such as palm oil.

[1]Department of Geographical Sciences, University of Maryland, College Park, MD 20740, USA. [2]College of Environmental Science and Forestry, State University of New York, Syracuse, NY 13210, USA.
*Corresponding author. Email: atyukav@umd.edu

Table 1. Food production and trade indicators. Data source: FAOSTAT Database (http://www.fao.org/faostat). Food production index 2014 (2004 to 2006 = 100) shows the relative level of the aggregate volume of agricultural production for the year 2014 in comparison with the base period 2004 to 2006.

Country	Food production index 2014 (2004–2006 = 100), net per capita	Agricultural products export value base price per capita, 2013 ($ per person)	Agricultural products import value base price per capita, 2013 ($ per person)	Food aid shipments, 2014, per capita (kg per person)
CAM	126	26	38	0.6
CAR	95	2	7	6.1
DRC	78	0.2	8	1.0
EQG	90	—	—	—
GAB	73	28	215	—
RoC	82	2	58	1.8
Brazil	123	263	24	—
Indonesia	125	78	35	—

The present study uses a sample-based analysis to estimate the rates of forest disturbance in Congo Basin countries between 2000 and 2014 and to attribute direct land use drivers to forest loss in different forest types. "Forest" is defined in the current study as any woody vegetation exceeding 5 m in height and 25% in canopy cover at a 30-m resolution (see the "Definitions" section). Global-scale (14, 15) and national-scale (16) wall-to-wall forest change maps provide diagnostic information on the extent of land cover change in forests. However, all maps contain errors and thus may underestimate or overestimate the area of forest change. For example, pan-tropical sample-based studies (17, 18) report almost twice as much gross tree cover loss in Africa in 2000 to 2010 compared to the Hansen et al. map (14) for the same time period, indicating significant map omission errors. Per good practice recommendations, land cover change area estimates should be derived from a probability sample of reference data (19, 20) rather than from counting map pixels, where reference data are defined as the best practically available assessment of ground condition. Following this guidance, the current study uses a stratified sampling approach to estimating forest loss area, with the Hansen et al. (14) global forest loss map used to construct strata to improve precision of the estimates (see Materials and Methods). A probability sample of ground observations performed within months of detected forest disturbance events and follow-up visits in the subsequent years would have been ideal to determine the initial direct driver of forest loss and possible future land cover and use transitions. This method was prototyped by our team in a series of rapid ground surveys in the Mexican Yucatan and Argentina. In the Congo Basin, however, such ground visits are less feasible due to the lower quality and coverage of the road network and safety concerns. The analysis of time series of all available Landsat observations for the study period supplemented with detailed very high resolution (1 m or better) imagery implemented in the current study is a more cost-efficient alternative to ground surveys. Previous pan-tropical studies of direct drivers of forest loss rely primarily on national reports and literature reviews (21, 22), which may be affected by inconsistent definitions, national politics, and poor quality of underlying data. Existing regional loss driver studies in the Congo Basin have used case study reviews (5), statistical analysis of auxiliary geospatial data sources (7, 23), and interviews with experts (2), all of which might also be affected by methodological inconsistencies and data quality issues. Using remotely sensed imagery directly to derive information on direct drivers of forest loss eliminates some of these issues and allows estimating loss drivers across national borders using the same data, method, and definitions. We first prototyped this approach in the Brazilian Legal Amazon (24) by identifying direct forest disturbance drivers and predisturbance forest types from a sample of 10,000 Landsat pixels.

Direct drivers of forest disturbance in this study are defined as human activities or biophysical events that directly affect forest cover and lead to canopy loss. Some direct drivers are distinguished using remote sensing data relatively easily (e.g., road construction, settlement expansion, mining, industrial selective logging, wildfires, and river meandering). For other drivers, such as the clearing of forest for agricultural activities, it is more difficult to identify the specific type of activity in the absence of information on land tenure (smallholders versus industrial enterprises), type of crop or livestock (subsistence versus commercial), and fallow cycle length. In these cases, we use a set of criteria distinguishable in satellite imagery, such as size of individual clearing (small-scale versus large-scale clearing of agriculture as a proxy to smallholder versus industrial agriculture) and presence/absence of forest regrowth (to distinguish between semipermanent and rotational agriculture). Less common clearing of forests for charcoal production is included in the "small-scale clearing for rotational agriculture" class, since the size of clearings and regrowth patterns of the two classes are similar and often colocated. Of direct drivers associated with forest degradation, we are able to detect only industrial selective logging and stand-replacement fires but cannot quantify the area affected by low-intensity artisanal logging, fuel collection, undercanopy livestock grazing, and low-intensity fires not resulting in significant canopy loss.

Distinguishing forest loss by predisturbance forest type is important because forests differ significantly in their carbon storage and biodiversity value. It is particularly significant to distinguish between high conservation value primary forests and secondary forests, which are a part of a shifting cultivation cycle. Most of the previous sample-based studies do not differentiate primary and secondary forests (7, 23). FACET (Forêts d'Afrique Centrale Evaluées par Télédétection) atlases distinguish primary and secondary forests and woodlands, but exist

only for DRC and RoC (http://carpe.umd.edu/carpemaps/) and therefore can only be used as stratifiers in national-level, sample-based studies (25). The Hansen et al. (14) global forest loss map, which is a stratifier in the current study, has been criticized for not distinguishing between types of tree cover (26). We have addressed this concern in past sample-based studies first by distinguishing between natural and human-managed forests (17) and later by using a more detailed classification of forest types (24). The forest type classification in the current study follows the more detailed classification approach and includes the following five types of predisturbance forest cover (see the "Definitions" section; fig. S2): (i) primary and mature secondary dense HTFs, (ii) young secondary dense HTFs, (iii) primary woodlands and dry forests, (iv) secondary woodlands and sparse secondary HTFs, and (v) tree and palm plantations.

To summarize, the objectives of the current study are the following: (i) estimate 2000 to 2014 forest loss area in the six Congo Basin countries and temporal loss trends using a recommended good practice probability sampling approach; (ii) identify direct drivers of forest disturbance distinguishable in remote sensing imagery using the same data, method, and definitions across national borders; and (iii) compare annual rates of forest disturbance in different forest types across the region.

RESULTS

The estimated 2000 to 2014 forest loss area in the study region is 16.6 ± 0.5 Mha (million hectares ± 1 SE) (table S2A). DRC alone contributes a higher percentage of forest loss than the other five countries combined (69.1 ± 1.7%), followed by CAM (9.9 ± 1.2%), RoC (8.2 ± 1.2%), CAR (7.4 ± 0.8%), GAB (4.7 ± 0.9%), and EQG (0.7 ± 0.2%). The average estimated annual area of forest clearing at the national level thus ranges from almost 1 Mha in DRC (817 ± 28 thousands ha) to about ten thousand hectares in EQG (8 ± 3 thousands ha).

Forest cover loss by direct driver

Small-scale forest clearing for agriculture is the largest direct driver of forest disturbance in the region, contributing about 84% of the total 2000 to 2014 forest loss area (table S2A). This includes clearing for rotational agriculture (82.1 ± 1.8%) and semipermanent conversion of woody vegetation into cropland (2.1 ± 0.5%), both of which could represent subsistence farming or production of commercial crops (27). Small-scale forest clearing is likely nonmechanized, which is supported by the size of individual clearings (median annual small-scale clearing size is estimated at 1.8 ha) and the lack of access roads visible in very high resolution imagery. At the national scale, small-scale clearing for agriculture is the main direct disturbance driver in all countries except GAB (Fig. 1). In DRC and in CAR, more than 90% of all forest loss is due to small-scale clearing for rotational agriculture. Semipermanent conversion to cropland is much less common than rotational agriculture, with CAM being the only country in which this conversion comprised more than 10% of the total forest disturbance area.

Large-scale clearing for agriculture (annual clearing size, >10 ha) constitutes only about 1% (0.9 ± 0.2%) of the overall forest loss area (table S2A and Fig. 1). This type of clearing, which is likely mechanized, includes forest clearing for tree and palm plantations and industrial pastures. CAM is the leading contributor to large-scale agro-industrial clearing of the region (56.5 ± 9.4%), followed by DRC (21.3 ± 7.4%), GAB (11.5 ± 5.4%), RoC (8.5 ± 7.9%), and EQG (2.2 ± 2.1%). Agro-industry in the region has been experiencing a new wave of develop-

ment since 2004 (11). Therefore, large-scale agro-industrial clearing is likely to become a more significant contributor to forest loss in the future.

Construction accounts for about 1.5% of forest loss in the region, which includes residential and commercial (1.0 ± 0.3%) and road (0.4 ± 0.1%) construction (table S2A and Fig. 1). The largest contribution of construction to forest loss on the national level is observed in EQG (18.7% of the national forest loss area), which is likely related to the country's large development projects of the last decade, such as construction of the new capital city of Oyala (28).

Mining is a very rare forest disturbance driver, accounting for only 0.04 ± 0.03% of the total forest loss area in the region. The estimate of forest loss area due to mining has low relative precision (SE expressed as percentage of driver area is 71%) because it is based only on two sampled pixels: one in EQG and one in CAR. Quantifying forest loss in the Congo Basin due to mining with high relative precision would require a stratification specific to mining, for example, a combination of existing mining concession boundaries and areas of semipermanent bare ground gain, derived from remote sensing. In absolute terms, the rarity of mining in our sample of 10,000 pixels gives us a good idea regarding the magnitude of the forest loss due to mining (the 95% confidence interval does not exceed 14,736 ha).

Industrial selective logging constitutes 9.5 ± 1.6% of forest loss area in the region (table S2A and Fig. 1). The largest contributors are RoC (39.5 ± 9.0%), GAB (30.7 ± 8.4%), and CAM (22.8 ± 7.9%), followed by DRC (6.2 ± 4.6%) and CAR (<1%). Area affected by industrial selective logging is defined using a 120-m buffer around logging damage and roads visible in Landsat imagery (see Materials and Methods), and therefore, the industrial selective logging area estimate is likely conservative. Selective logging does not imply complete canopy loss and hence does not result in the same carbon emissions as stand-replacement forest disturbance drivers, which should be taken into consideration when interpreting the carbon implications of the current area estimates.

Fires, resulting in the loss of canopy, but not followed by agricultural activities, account for 3.8 ± 1.0% of forest loss area in the region (table S2A and Fig. 1). These are likely escaped agricultural fires or fires set for hunting purposes: 78% of the sampled pixels identified as "fire" were adjacent to the forest edge and human activities (roads, settlements, and active fields). DRC contributes most of the region's fire disturbance (78.8 ± 7.4%), followed by RoC (8.4 ± 4.4%), CAR (6.7 ± 3.5%), CAM (3.7 ± 2.4%), and GAB (2.4 ± 2.4%). Natural forest disturbances, including windfalls and river meandering, contribute only about 0.13 ± 0.07% to the total forest loss area.

Forest cover loss by predisturbance forest type

Forest loss in primary and mature secondary dense HTFs in 2000 to 2014 accounts for 43.7 ± 1.7% of forest loss area in the region (table S2A), followed by clearing in young secondary dense HTFs (34.9 ± 1.6%), primary woodlands and dry forests (16.8 ± 1.4%), secondary woodlands and sparse secondary HTFs (4.2 ± 0.8%), and tree plantations, established by the year 2000 (0.4 ± 0.1%). At the national scale, clearing of primary and mature secondary dense HTFs is prevalent in GAB, RoC, and CAM (Fig. 2). The extent of loss of primary and mature secondary dense HTFs in DRC is comparable to the reclearing of young secondary dense HTFs (Fig. 2), which indicates the presence of large established shifting cultivation areas. Forest loss in CAR occurs mainly within primary woodlands and dry forests. EQG has the lowest proportion of forest loss within primary vegetation among all countries (Fig. 2).
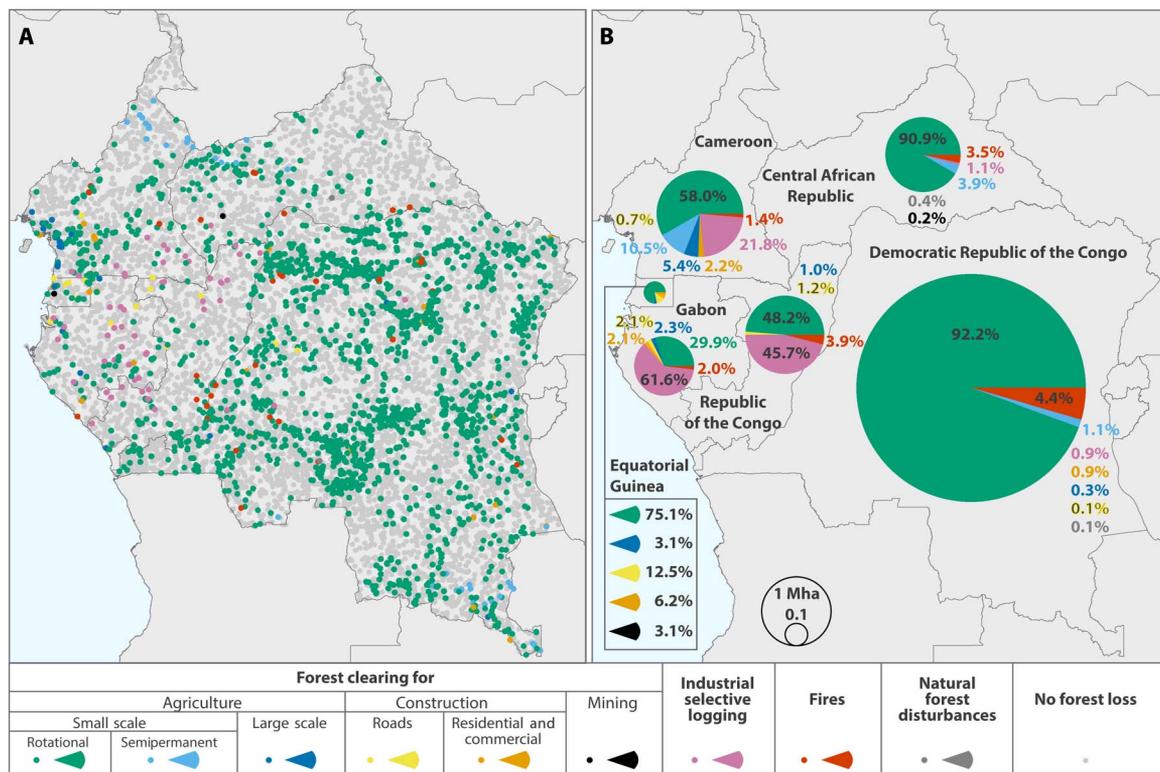
Fig. 1. Forest disturbance driver. (**A**) Reference disturbance driver for each sampled pixel. (**B**) National estimates of 2000 to 2014 forest loss area by disturbance driver. Area estimates along with SEs are presented in table S2A. Forest clearing for small-scale rotational agriculture includes clearing for charcoal production, the contribution of which does not exceed 10% of the class area (*42*).

Within primary and mature secondary dense HTFs, 70.3 ± 3.2% of forest loss is due to small-scale clearing for rotational agriculture (table S2A), which is an indication of shifting cultivation expanding into previously undisturbed forest. This finding is consistent with Molinario *et al*. (*29*), who found that the area under shifting cultivation and rural settlements in DRC grew by 10% between 2000 and 2010. Selective logging is also a significant contributor to primary and mature secondary dense HTF loss (21.7 ± 3.2%), followed by fire (5.8 ± 1.8%), large-scale agro-industrial clearing (1.3 ± 0.3%), and road construction (0.5 ± 0.2%).

Young secondary dense HTFs and secondary woodlands and sparse secondary HTFs are cleared almost exclusively in the context of small-scale rotational agriculture (97.8 ± 0.5% and 95.9 ± 2.3%, respectively; table S2A). Primary woodlands and dry forests are cleared for both rotational (78.0 ± 4.3%) and semipermanent agriculture (12.5 ± 2.9%). Old tree plantations are either cleared and replanted again (68.6 ± 16.0%) or converted to small-scale shifting cultivation (31.4 ± 16.0%).

Temporal trends of forest loss

Annual forest loss trends are analyzed at a regional scale by disturbance driver and predisturbance forest type (table S2B and Fig. 3). Among the major disturbance categories (Fig. 3), small-scale clearing for rotational agriculture is increasing both in primary and mature secondary dense HTFs and in primary woodlands and dry forests. Accelerating rates of small-scale clearing in these forest types are likely linked to increasing population pressure (Fig. 4). However, at the national scale, not all countries display the same increasing trend of

small-scale clearing in primary forests and woodlands (Table 2). In GAB, where industrial selective logging accounts for more forest loss than small-scale clearing for agriculture (Fig. 1), encroachment of small-scale agricultural activities into primary forests and woodlands has slowed down by 2014 (Table 2). In CAR, small-scale clearing for agriculture in primary forests and woodlands first accelerated and then slowed down again (Table 2), possibly because of the civil war, which started in 2012.

Small-scale forest clearing for rotational agriculture in secondary forests displays a decreasing trend (Fig. 3), which is explained by the way young secondary forests are defined in the current study (see the "Definitions" section and Discussion). Industrial selective logging in primary and mature secondary dense HTFs peaked at the beginning and at the end of the study period (Fig. 3). Lower logging rates in 2007 to 2008 may be linked to the decreased demand for timber during the global financial crisis (*30*).

DISCUSSION
Drivers of forest disturbance
Results of the current study provide a quantitative assessment of regional socioeconomic drivers resulting in forest loss. Congo Basin forests are being cleared primarily by manual means: Nonmechanized small-scale forest clearing for agriculture is responsible for 84% of the total forest loss between 2000 and 2014. In the least-developed countries, DRC and CAR, small-scale clearing is even more dominant (more than 90%). The dominance of local populations and subsistence farming within the Congo Basin distinguishes it from deforestation
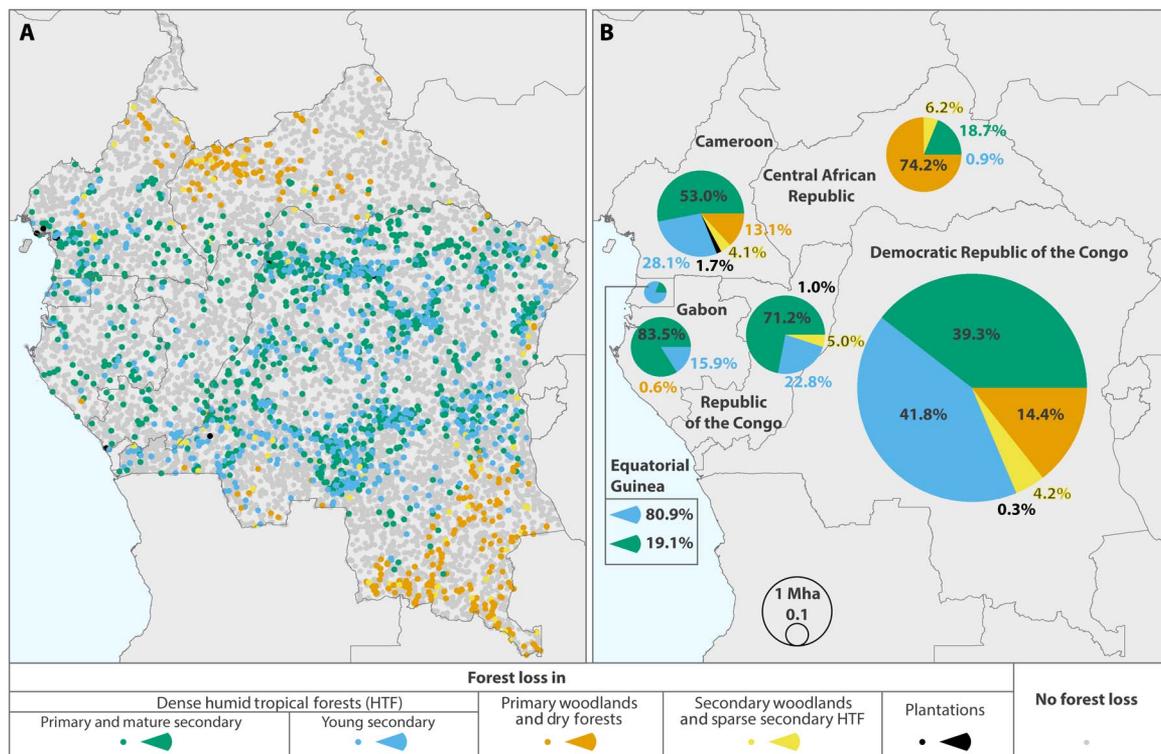
Fig. 2. Predisturbance forest type. (**A**) Reference predisturbance type for sampled pixels identified as forest loss. (**B**) National estimates of 2000 to 2014 forest loss area by predisturbance forest type. Area estimates expressed in hectares along with SEs are presented in table S2A.

dynamics in the Amazon Basin and Insular Southeast Asia. The Congo Basin has historically lagged the Amazon Basin and Insular Southeast Asia, the world's other large remaining HTF regions, in the amount and rate of tropical forest clearing. Table 1 includes data for Brazil and Indonesia, the countries with the highest deforestation totals in recent history, and illustrates dramatically increasing food production and agricultural export totals compared to the underdeveloped economies of the Congo Basin. Agro-industrial land use drivers of clearing in Brazil are mainly pasture for cattle production and cropland for soybean cultivation (*31*). In Indonesia, palm oil and forestry are the principal land uses replacing primary forests (*32*). While agro-industrial clearing has not been significant in the Congo Basin, there is nascent large-scale clearing of forests for palm oil (*11*). For DRC, where smallholder farming predominates, the main implement for clearing forests remains the axe. From 2010 to 2014, the area of primary forest clearing in DRC was equivalent to 54% of Indonesia's and 46% of Brazil's area of primary forest clearing (*33*). The fact that DRC's clearing is largely by hand and still equal to roughly one-half that of the two dominant deforestation countries is an indication of the scale of smallholder cropland expansion in DRC.

The low level of development and political instability in the two smallholder-dominated forest loss countries, DRC and CAR, is reflected in forest clearing rates that are largely correlated with population growth. Resulting population pressure on land resources can lead to environmental degradation in efforts to produce sufficient food (*34*). The increasing rate of forest loss due to smallholder agriculture reflects the lack of agricultural intensification in the Congo Basin, which could compensate for increasing population densities (*35, 36*). Alternatives to shifting cultivation practices are of particular importance given growing populations, especially in DRC. Expected population growth is due to

persistently high fertility levels and increasing longevity. Recent United Nations' population projections for DRC estimate 197 million people by 2050 and 379 million by 2100, when DRC is expected to be the fifth most populous country in the world. Under the assumption that population growth continues to correlate with the increase in annual primary forest loss area, all of DRC's primary forests will have been cleared by 2100. The strategy for survival in DRC is best reflected in the concept of "Article 15," the popular and imagined 15th article to the 14-article constitution of the 32-year Mobutu dictatorship. Article 15 means "figure it out" and represents "an implicit social pact between the state and its citizens since it allowed the former [the state] to retire from public life and from its functions" (*37*). The practical outcome has been self-reliance in nearly every aspect of life for the citizens of DRC. Since the end of the Mobutu regime, the ongoing conflict within DRC has only exacerbated the challenges of DRC residents, with escalating hunger and malnutrition due to prolonged conflict and displacement (*38*). In terms of land cover and land use change, self-reliance in response to statelessness is evident in elevated forest disturbance rates compared to other Congo Basin countries, as the entire rural population attempts to eke out a subsistence livelihood. The fate of remaining HTFs in DRC will be a function of alternative development strategies given a daunting population growth trajectory.

The likely expansion of agro-industrial development will add to the demographic challenge. Agro-industrial clearing was found primarily in the Gulf of Guinea countries with 70% of the total 2000 to 2014 large-scale clearing for agriculture occurring after 2007 (table S2B). Annual rates of industrial selective logging in primary and mature secondary dense HTFs have also been steadily increasing since 2007 (Fig. 3). This indicates that while subsistence agriculture is still the leading driver of forest loss in the region, future industrial development
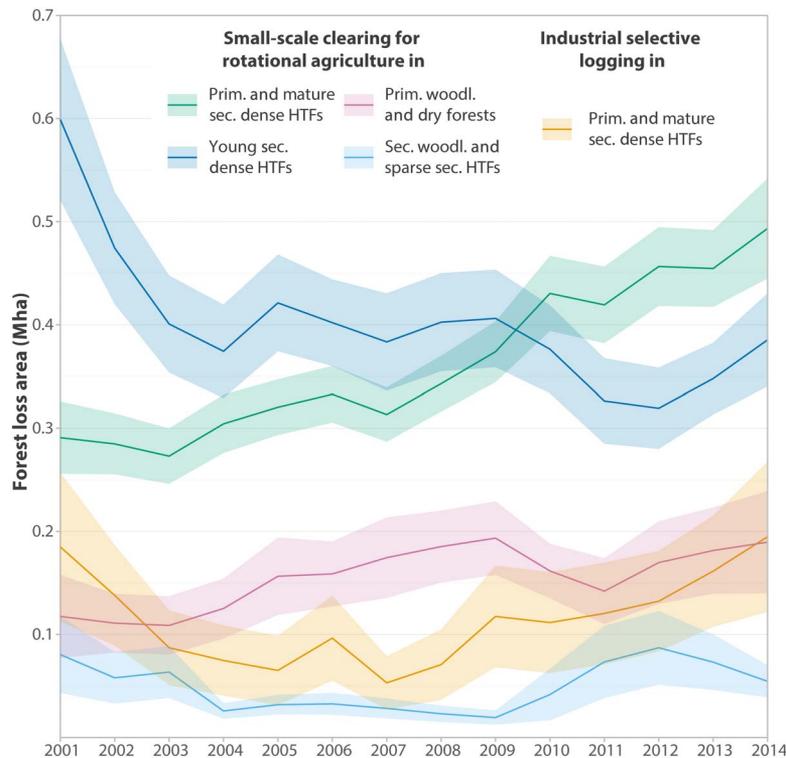
Fig. 3. Three-year moving average of annual forest loss area for the major disturbance categories in all countries. Each major disturbance category contributes >0.5 Mha to the total 2000 to 2014 forest loss area. Forest clearing for small-scale rotational agriculture includes clearing for charcoal production, the contribution of which does not exceed 10% of the class area (*42*). Error bands represent ±SE. Annual area estimates along with SEs are presented in table S2B. Prim., primary; sec., secondary; woodl., woodlands.

will bring new challenges to forest resources management. For example, development of infrastructure for resource extraction and agro-industry will likely facilitate encroachment of subsistence agriculture into previously undisturbed (intact) forest areas. Potapov *et al.* (*39*) illustrated several dynamics associated with the expansion of certified sustainable logging in the northern RoC, including expanding agriculture around logging towns and increased infrastructure, such as paved roads and a dam for hydroelectric power generation. Increasing infrastructure development investment from China, India, and the Gulf states in the recent years (*40*) may accelerate this process. Land use planning that minimizes the conversion of natural forest cover for agro-industry will serve to mitigate this nascent and growing threat to primary forests.

Temporal disaggregation of forest loss in different forest types presented in the current study provides definitive information on forest loss trends in the region. For example, the Hansen *et al.* (*14*) global forest loss map underestimates forest loss area in the early 2000s and overestimates forest loss in the 2010s, as demonstrated for the Congo Basin (current study, fig. S7) and for the Brazilian Legal Amazon (*24*). Disaggregation of forest loss area by disturbance driver and predisturbance forest type provides context to previous forest loss estimates. From previous studies (*16, 17, 25*), the total estimated area of secondary forest loss in DRC for the 2000 to 2010 and 2000 to 2012 intervals exceeds the total area of primary forest loss to a greater degree than the presented 2000 to 2014 study (Fig. 3), reflecting increasing clearing of primary forests over time and decreasing pool of year 2000 secondary forests available for reclearing. The annual rates and general trend of primary forest loss in DRC agree with Turubanova *et al.* (fig. S7). Ernst *et al.* (*23*) reported increasing rates

of deforestation between 1990 to 2000 and 2000 to 2005 in dense forests of all countries except GAB (EQG not reported). While these results are not directly comparable with the current estimates owing to different definitions and study period, we observed similar national trends of small-scale clearing for agriculture in primary forests and woodlands between 2000 and 2014 (Table 2). Comparison of the studies mentioned above and the FAO FRA 2015 (Global Forest Resources Assessment 2015 of the Food and Agriculture Organization of the United Nations) report (*41*) with the current results for DRC is presented in table S3.

Limitations

Direct assessment of disturbance drivers from remote sensing data is advantageous in providing relative objectivity and consistency across national borders. The legend is easily adaptable to include region-specific drivers when applying the method in a different geographic domain or globally. However, there are limitations in how much thematic detail can be interpreted. For example, we were not able to distinguish small-scale clearing for agriculture from forest clearing for charcoal production, which may be colocated with the establishment of new agricultural fields. Charcoal production is estimated to account for up to 10% of forest loss in DRC and CAM (*42*). While fuel wood collection in rural areas is largely offset through forest regeneration, demand for energy from urban areas can lead to forest degradation and deforestation. Charcoal is the fuel of choice in urban settings as it is easier and cheaper to transport and store and produces more energy per unit mass compared to wood. The Congo Basin's largest city, Kinshasa, sources charcoal within a 200-km radius with negligible
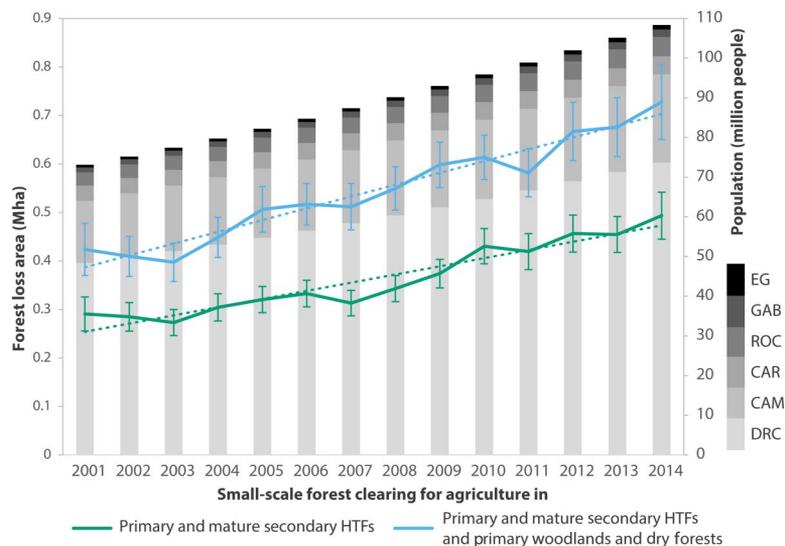
Fig. 4. Expansion of small-scale agriculture into recently undisturbed forests and woodlands (lines) and population growth in the region by country (bar chart). Solid lines connect the annual forest loss area estimates and dashed lines represent the linear trend based on ordinary least squares regression. Forest clearing for small-scale rotational agriculture includes clearing for charcoal production, the contribution of which does not exceed 10% of the class area (*42*). Error bars on the area estimates represent 1 SE.

Table 2. Annual area of small-scale forest clearing for agriculture in primary and mature secondary dense HTFs and primary woodlands and dry forests (thousand hectares ± SE) by 5-year epochs. Forest clearing for small-scale rotational agriculture includes clearing for charcoal production, the contribution of which does not exceed 10% of the class area (*42*). EQG had only 20 sampled pixels identified as forest loss, and this small sample size did not yield adequately precise estimated annual loss rates by 5-year epochs.

	2000–2005	2005–2010	2010–2014
DRC	321 ± 26	403 ± 27	462 ± 33
CAR	64 ± 17	88 ± 20	80 ± 12
CAM	28 ± 7	37 ± 7	69 ± 16
RoC	9 ± 3	24 ± 8	35 ± 9
GAB	17 ± 5	7 ± 3	4 ± 2

contributions from wood energy plantations (*5*). Improved spatial disaggregation of charcoal as a driver of forest loss is needed.

Other drivers such as mining were virtually absent in the sample population, reflecting their relative rarity compared to smallholder agriculture. Given that the stratification is guided by observed forest disturbance, rare land change drivers will not be well represented in the analysis as SEs relative to the rare class area will often be large. For rare classes, the 95% confidence interval establishes a useful upper bound because it identifies that the change driver comprises "at most" this percentage of the total loss. For example, at a 95% confidence level, the true proportion of forest loss due to mining is at most 0.1% of the total loss area of the region (<0.015 Mha), natural forest disturbance is at most 0.3% (<0.044 Mha), road construction is at most 0.7% (<0.11 Mha), large-scale clearing for agriculture is at most 1.3% (<0.21 Mha), and commercial and residential construction is at most 1.6% (<0.26 Mha). One approach to targeting rare drivers more direct-

ly is by mapping forest disturbances by driver, which is often required by countries for land use planning. Spatially explicit mapping of forest disturbance drivers could be then supplemented with sample-based analysis, providing map accuracy information and unbiased area estimates. We have prototyped such approach to map forest conversion to cropland in Brazil, but in the context of small-scale forest dynamics of the Congo Basin, direct mapping of disturbance drivers may be more challenging. Regardless, forest loss map information used in the current study to target sample allocation through stratification significantly increased precision of the estimates compared to simple random sampling. For example, a simple random sample of 10,000 pixels would have yielded a 4.8% SE of the total 2000 to 2014 forest loss area estimate in the region, compared to the stratified SE of just 3.2%, resulting in a 33% reduction of uncertainty. For estimates of individual loss drivers and forest types, we observed reductions in uncertainty from stratification to be as much as 72% relative to the SE of simple random sampling.

Estimating temporal trends of small-scale forest clearing for rotational agriculture in secondary forests is limited by the way the young secondary forests are defined in the current study. We consider a sampled pixel forested if it had forest cover in the year 2000; therefore, fallows that reached a 5-m height threshold after 2000 and were later cleared were not considered forest loss in this study. We therefore end up with a limited pool of young secondary forests in the areas of subsistence agriculture, which are recleared on average every 18 years (*43*). By the end of our 14-year study period, most of the year 2000 young secondary forests would have been cleared, resulting in decreasing rates of clearing for this forest type. Including forest gain into the assessment would have helped address this issue and track changes in young secondary forests that regrew during the study period.

Future potential advances
Forest type definitions are always a matter of debate and a source of thematic uncertainty in forest loss area estimation. Using canopy structure characteristics (% cover, height, and biomass density) and disturbance history to define forest types may help reduce such

thematic uncertainty (17) and enable global applications of the method. Forest type as defined in the current study is based on an objective criterion of canopy density, which is modeled from optical remote sensing data. Landsat-modeled canopy height was used as one of the quality checks for forest type definition (table S4). In the future, improved global light detection and ranging (LIDAR) data, for example, from the proposed NASA Global Ecosystem Dynamics Investigation mission, will advance direct mapping of canopy height and other structural metrics into forest definitions. Forest age and absence of disturbance (e.g., "primary and mature secondary forests" versus "young primary forests") are somewhat harder to define and measure. Primary and intact forest maps, derived using direct and indirect mapping methods (33, 39, 44), could be used to supplement sample-based analysis.

Systematic acquisitions of high-frequency, very high spatial resolution images, a capability currently being developed by commercial companies such as Planet (45), may be an option for improving reference data. However, generic data access to such data sources by the scientific and natural resource management communities is not a given. Even with dense time series of very high resolution data readily available, visual assessment of gradual processes such as forest regrowth or degradation will be challenging. Gradual forest changes can be modeled on the basis of the spectral response from the canopy, but validation data for these models will have to come from multiyear ground observations or time series of airborne LIDAR data measuring small changes in canopy structure. Therefore, we currently only focus on quantifying gross forest loss from disturbance events resulting in canopy damage and do not aim to produce net forest change estimates or to quantify the extent of forest degradation. We do, however, include industrial selective logging, which is usually considered a type of forest degradation, into the assessment of forest disturbance drivers. Because of the definition used (120-m buffer around visible logging damage), our estimates of area affected by selective logging are likely to be considerably more conservative compared with the estimates derived by outlining the polygons of forests encompassing logging damages (46).

Attempts have been made to establish global reference data sampling frames to validate global tree cover maps (47) and estimate the area of different land cover types (48). These sampling frames that use stratified random or systematic sampling with strata being biomes or ecoregions are useful for the assessment of stable land cover classes. In the case of small dynamic land cover change classes, such as forest loss (49) or bare ground gain (50), stratification should be targeting these dynamics directly to ensure higher sampling efficiencies and lower uncertainty of area estimates. Online tools for reference data collection, such as Collect Earth (51), enable leveraging regional knowledge of image interpretation experts from around the world and transferring technical capacity to the institutions in developing countries responsible for national land cover change reporting. Sample size required for global assessments will depend on desired precision of the estimates and on the scale of reporting (e.g., biome-level estimates versus national versus subnational).

Forest loss area estimates, or activity data, enable carbon emissions reporting (52). In the past, we have demonstrated two different approaches to combining sample-based area estimates similar to those derived in the current study with information on predisturbance forest biomass (emissions factors). In the first approach ("stratify and multiply"), sampling domains with minimized within-domain carbon density variance are created (17, 25), and a single mean carbon density value is assigned to the sample-based forest loss area estimate for each domain. In the second approach, existing continuous forest biomass maps are used to derive emissions factors per predisturbance forest

type class, identified from the sample (24). Although the current study does not have the objective of estimating carbon losses associated with forest loss, such estimates could easily be derived using emissions factors from existing continuous maps or other sources of regional or country-specific emissions factors.

MATERIALS AND METHODS
Definitions
Forest loss is defined in the current study as complete or partial removal of woody vegetation, which reached a 5-m height threshold by the year 2000 and >25% tree canopy cover, within a sampled 30 m by 30 m pixel. This includes "stand-replacement disturbance or the complete removal of tree cover canopy at the Landsat pixel scale," as defined by Hansen et al. (14), and partial tree cover losses associated with boundary pixels and selective logging. Forest loss was recorded in three gradations: 75 to 100% (counted as 100% of pixel area lost), 25 to 75% (50% of pixel area lost), and <25% (0% of pixel area lost). These coarse gradations were distinguishable in Landsat, which was the primary source of the reference data (i.e., the observations used to produce the area estimates) (fig. S1). The partial loss category includes pixels located on the edges of 2000 to 2014 forest disturbance patches (example: DRC sample 2615 at http://glad.umd.edu/CAFR) and pixels located on the boundaries of forest patches in the year 2000 that have undergone complete clearing of tree cover between 2000 and 2014 (example: Cameroon sample 118 at http://glad.umd.edu/CAFR).

Forest loss year is defined as the year of the maximum percent canopy cover removal. For example, if, initially, the sampled pixel was cleared only partially and was later fully cleared, only the last year was recorded as the loss year. When multiple complete or partial vegetation clearing events occurred within the study period (2001 to 2014), only the first complete clearing event was recorded.

Predisturbance forest categories include the following (fig. S2): (i) primary and mature secondary dense (>60% tree canopy cover) HTFs, (ii) young secondary dense HTFs, (iii) primary woodlands (25 to 60% tree canopy cover) and dry forests (>60% tree canopy cover, presence of dry season), (iv) secondary woodlands and sparse (25 to 60% tree canopy cover) young secondary HTFs, and (v) plantations. We did not use a minimal patch size in defining forest; instead, we defined forest at the Landsat pixel scale as woody vegetation exceeding 5 m in height and 25% in canopy cover. Quantitative thresholds of the visually interpreted forest type classes were verified using existing Landsat-based tree cover (14) and height (53) models. Height models were reported to overestimate the height of tree cover <5 m (mean absolute error of about 1.6 m), which may lead to inclusion of some vegetation under 5 m into woodland classes in the current study. Mature secondary dense HTFs are defined as disturbed in the past, but not distinguishable from the never disturbed primary dense HTFs in year 2000 Landsat imagery. Field evidence suggests that tropical secondary forests restore structure and species richness similar to those of primary forests after about 40 years (54). Young secondary dense HTFs are mainly associated with the shifting cultivation areas, and these forests have a distinct spectral signature (fig. S2B) and lower canopy heights compared to primary and mature secondary HTFs. Primary woodlands and dry forests represent natural vegetation outside HTF zones and are characterized by distinct seasonality. Secondary woodlands and sparse young secondary HTFs represent the sparse woody vegetation regrowth both in HTF and in woodland zones. The plantation category represents palm and tree plantations, established by the year 2000.

Forest disturbance drivers include four broad categories: human forest clearing, industrial selective logging, fires, and natural disturbances (Fig. 1 and fig. S3). Human forest clearing includes clearing for agriculture, clearing for construction, and clearing for mining.

Clearing for agriculture includes small- and large-scale clearing categories. Large-scale clearings for agriculture have area of annual clearing exceeding 10 ha; these are industrial mechanized clearings for plantations and pastures (fig. S3C). Small-scale clearings have a median annual clearing size of 1.8 ha (about 5 by 5 Landsat pixels), which was estimated on the basis of manually digitized annual clearing patches from Landsat composites for a random sample of 100 pixels identified as "small-scale clearing." Small-scale clearing for agriculture was further distinguished into clearing for rotational (fig. S3A) and semipermanent (fig. S3B) agriculture. Small-scale clearing for rotational agriculture was characterized by forest regrowth starting 3 to 4 years after the clearing; for the clearings at the end of the study period (after 2011), this driver was assigned on the basis of the regrowth dynamics of the neighboring clearings. This disturbance category includes clearing for charcoal production, which cannot be reliably distinguished from slash-and-burn agriculture in the absence of very high resolution imagery temporally colocated with charcoal burning. Small-scale clearing for semipermanent agriculture was distinguished from rotational agriculture by the absence of forest regrowth in the years following the clearing.

Forest clearing for construction includes road (fig. S3D), residential (fig. S3E), and commercial (fig. S3F) construction. The road construction category does not include roads that are the part of selective logging infrastructure. Semipermanent roads, included in this category, were distinguished from logging roads by the absence of forest regrowth and presence of settlements and agricultural activities along the roads. Residential construction and commercial construction were treated as one class, since the absence of very high resolution imagery for some sampled pixels would not allow consistently distinguishing these construction types.

Forest clearing for mining is defined as removal of woody vegetation in the process of mineral resources extraction (fig. S3G). This category is characterized by the spectral signature of bare ground without significant regrowth following forest disturbance, similar to that of construction.

Industrial selective logging is defined as canopy damage resulting from logging infrastructure (logging roads, skid trails, and landings), distinguishable in Landsat resolution, and a 120-m buffer around this canopy damage to capture partial canopy loss associated with tree felling and transportation. A 120-m buffer was initially selected for a study in the Brazilian Legal Amazon (24) and was preserved in the current study for consistency of the estimates. The sampled pixel was labeled as "selective logging" if any visible logging damage was observed in a 120-m buffer around it (white circle, fig. S3H). This forest disturbance driver does not imply complete canopy loss within a sampled pixel. Fragmentation effects of industrial selective logging were not considered in the current study.

Forest loss from fire (fig. S3I) is defined as burning that was not followed by agricultural activities, unlike small-scale clearing for rotational agriculture. This includes areas affected by fires escaped from slash-and-burn agricultural practices and fires set for hunting purposes: 78% of the sampled pixels identified as "fire" were adjacent to the forest edge and human activities (roads, settlements, and active fields). We detected complete canopy loss in 72% of the sampled pixels identified as fire, whereas the rest (28%) were non–stand-replacement fires. Natural forest disturbances (fig. S3J) include river meandering, windfalls, and other forest disturbance events (droughts and insect outbreaks) that cannot be directly linked to human activities.

Sampling design

The study area consisted of the Congo Basin Forest Partnership countries: CAM, CAR, DRC, EQG, GAB, and RoC (fig. S4). To estimate forest loss area within this study region, we used a stratified sampling design, which typically yields better precision compared to simple random and systematic sampling designs (49, 55). Strata were selected to target forest cover loss (fig. S4) with the three strata defined as follows: (i) "Loss," any pixel that was mapped as forest loss during 2001 to 2014 where forest loss was determined from the global forest loss map [Hansen et al. (14)]; (ii) "Probable loss," 60-m (two Landsat pixels) buffer around mapped loss; (iii) "No loss," all other areas outside of mapped loss and the probable loss buffer (including both forested and nonforested areas). The sampling unit was one Landsat pixel (circa 30 m by 30 m); the mean pixel area within the study region in geographic coordinates (latitude/longitude) was 766.13 m². The variation of mean pixel area among the countries did not exceed 0.2% and was therefore ignored. The total number of sample pixels was 10,000, with 20% of the sample randomly allocated to the "Loss" stratum, 30% to the "Probable loss" stratum, and 50% to the "No loss" stratum. Pixels were allocated to the three sampling strata regardless of country boundaries. Countries were treated as poststrata in the area calculations. The resulting distribution of sample pixels among the countries (poststrata) and three sampling design strata is shown in table S5.

Estimation of area from the sample was performed using indicator functions (56), since this approach works when the sampling strata are different from the map classes and can also be used for the nonbinary (proportional) reference sample labels (in our case, 0, 50, and 100% forest loss). Forest loss area for each reference forest loss type (by disturbance driver, by predisturbance forest type, and by year), reported in table S2, was estimated using the following equation

$$\hat{A} = A_{\text{tot}} * \sum_{h=1}^{H} \frac{N_h}{N} \bar{y}_h \tag{1}$$

where A_{tot} is the total study region area, N is the total number of pixels in the study region, H is the number of poststrata (18, see table S5), n_h is the sample size (number of sampled pixels) in poststratum h, N_h is the total number of pixels in poststratum h, y_u is 1 or 0.5 if pixel u (or its half) is classified as "forest cover loss" in the reference sample interpretation and y_u is 0 otherwise, and $\bar{y}_h = \frac{\sum_{u \in h} y_u}{n_h}$ is the sample mean of the y_u values in poststratum h.

To produce forest loss area estimates by disturbance driver, predisturbance forest type, and year, the definition of y_u is modified so that 1 or 0.5 is recorded only if the loss area represents the specified disturbance driver, predisturbance forest type, or year targeted by the estimate, and $y_u = 0$ if there is no forest cover loss or the sampled pixel u does not satisfy the definition of the target subset. The SE of the sample-based loss area estimate is

$$\text{SE}(\hat{A}) = A_{\text{tot}} * \sqrt{\frac{\sum_{h=1}^{H} N_h^2 \left(1 - \frac{n_h}{N_h}\right) \frac{s_{yh}^2}{n_h}}{N^2}} \tag{2}$$

where $s_{yh}^2 = \frac{\sum_{u \in h} (y_u - \bar{y}_h)^2}{n_h - 1}$ is the sample variance for poststratum h.

When estimating the relative contribution of each loss driver, forest type, or country to the total area of forest loss, expressed as percentage, both numerator and denominator are estimated from the sample, resulting in a ratio estimator. Other examples for which a ratio estimator is required include the estimates of contribution of each country to the total area of forest loss of each driver, and the estimates of the contribution of each loss driver to the total area of forest loss of each forest type. The combined ratio estimator for stratified random sampling (57) was therefore used to estimate these percentages, reported in Results

$$\hat{R} = \frac{\sum_{h=1}^{H} N_h \bar{y}_h}{\sum_{h=1}^{H} N_h \bar{x}_h} \quad (3)$$

where $y_u = 1$ or 0.5 if pixel u (or its half) is classified as belonging to a specific driver, forest type, or country in the reference sample interpretation, and $y_u = 0$ otherwise; $x_u = 1$ or 0.5 if pixel u (or its half) is classified as forest cover loss in the reference sample interpretation, and $x_u = 0$ otherwise; $\bar{y}_h = \frac{\sum_{u \in h} y_u}{n_h}$ is the sample mean of the y_u values in poststratum h; and $\bar{x}_h = \frac{\sum_{u \in h} x_u}{n_h}$ is the sample mean of the x_u values in poststratum h.

The SE of the combined ratio estimator is

$$\mathrm{SE}(\hat{R}) = \sqrt{\frac{1}{\hat{X}^2} \sum_{h=1}^{H} N_h^2 \left(1 - \frac{n_h}{N_h}\right) \left(s_{yh}^2 + \hat{R}^2 s_{xh}^2 - 2\hat{R} s_{xyh}\right) / n_h} \quad (4)$$

where $\hat{X} = \sum_{h=1}^{H} N_h \bar{x}_h$ is the estimated total area of tree cover loss expressed in pixels, s_{yh}^2 and s_{xh}^2 are the sample variances in poststratum h, and $s_{xyh} = \frac{\sum_{u \in h} x_u y_u - n_h \bar{x}_h \bar{y}_h}{n_h - 1}$ is the sample covariance in poststratum h.

Sources and availability of reference data
The primary source of reference data for the visual interpretation of sampled pixels was Landsat data in the form of cloud-free annual composites and 16-day observations (http://glad.umd.edu/CAFR). Methods of Landsat data processing, cloud filtering, and compositing are described in Potapov et al. (58). Sixteen-day observations were cloud screened for the graphs of spectral indices (normalized difference vegetation index and normalized difference water index) and shortwave infrared band reflectance. Non–cloud-screened 16-day composites were used to identify the exact date of forest loss: Loss events are sometimes visible through haze and translucent clouds, which would have been removed in the automated process of cloud screening. To provide landscape context to the visual interpretation of sampled pixels, annual composites include a subset of 20 by 20 Landsat pixels (circa 36 ha) around the sampled pixel and 16-day composites include a subset of 40 by 40 Landsat pixels (circa 144 ha).

Regionally, only 7% of the 10,000 sampled pixels had, on average, less than one cloud-free Landsat observation per year (fig. S5A). These pixels were clustered in the cloudiest areas along the coast and over the HTFs in the core of the Congo Basin, introducing a spatial bias of data availability. Consistent with this regional pattern, the country mean of average number of cloud-free observations per year for each sampled pixel (fig. S5A) was 0.9 in EQG, 1.1 in GAB, 2.0 in RoC, 3.0 in CAM, 4.1 in DRC, and 4.7 in CAR. In all countries except EQG, the

majority of sampled pixels had, on average, one or more cloud-free observations per year, despite the large within-country variability of available data. From all sampled pixels, 56% did not have any years with zero cloud-free Landsat observations (fig. S5B), 20% had only one gap year, 9% had two gap years, 4% had three gap years, 2% had four gap years, and 9% had five or more gap years with zero cloud-free observations. Among the countries, EQG and GAB had the largest percentage of sampled pixels with at least one missing year (99 and 98%, respectively), followed by RoC (82%), CAM (53%), DRC (40%), and CAR (10%). This means that the error of forest loss occurrence and date identification due to the reference data availability was probably the highest in EQG and GAB and the lowest in CAR.

Landsat data availability also varied from year to year owing to the characteristics of the Landsat satellite program (fig. S5C). Year 1999 had the lowest data availability because Landsat 7 was launched in April 1999, and its predecessor Landsat 5 did not have a global data acquisition strategy. Year 1999 data were used only as a pre-2000 benchmark to help identify year 2000 forest cover; thus, the low availability of 1999 data did not affect our results directly. Lower data availability occurred in 2003 (fig. S5C) because of the malfunction of the Landsat 7 Scan Line Corrector. This likely resulted in some underestimation of the year 2003 forest loss. The number of available cloud-free observations increased in 2013 and 2014 after the launch of Landsat 8 (fig. S5C), which might have affected our interpretation results as well, leading to better detection of forest loss closer to the end of the study period.

The secondary source of reference data used primarily to help identify the initial forest cover and forest disturbance driver was very high resolution data from Google Earth. The link opening Google Earth for each sampled pixel is available from the interpretation interface (http://glad.umd.edu/CAFR). From all sampled pixels, 74% had at least one very high resolution (<1 m) image on Google Earth, 7% had image from SPOT satellite (2.5 m resolution), and 19% had only Landsat.

Sample labeling protocol and confidence of reference interpretations
All 10,000 sample pixels were initially screened by two independent experts, who assigned forest loss (0, 50, or 100%) to each sample pixel. Pixels identified as 50 or 100% loss were attributed with loss year, pre-disturbance forest type, and forest disturbance driver (see the "Definitions" section). Experts also recorded their confidence (high/low) separately for the presence/absence of forest loss, forest loss year, pre-disturbance forest type, and forest disturbance driver. After the initial screening, sample pixels with disagreement between the two experts and pixels marked as "low confidence" for any interpretation category were additionally rechecked with the help of a third expert. Major sources of uncertainty during sample interpretation and the ways they were addressed by the interpreters are listed in table S4. Additional checks were performed using auxiliary data sources for the following pixels regardless of their initial confidence level:

(1) Primary and mature secondary HTF pixels with Landsat-modeled year 2000 tree cover <90% (14);

(2) Primary and mature secondary HTF pixels with Landsat-modeled year 2000 tree cover (14) >90% and year 2000 tree cover height (53) <15 m;

(3) Young secondary HTF pixels with Landsat-modeled year 2000 tree cover height (53) >20 m;

(4) Primary and mature secondary HTFs and primary woodlands and dry forest pixels in DRC outside primary forest mask (33);

(5) Young secondary HTFs and secondary woodland pixels in DRC within primary forest mask (33);

(6) Pixels with forest loss year 3 or more years different from the global forest loss map (14).

Sample pixels were iteratively rechecked by interpreters using auxiliary data until consensus on the final pixel labels and confidence levels was reached.

Because we used the best available information for our reference sample classification (visual interpretation of Landsat time series and available very high resolution data), it is not possible to formally assess the accuracy of our reference classification by comparing it to the "truth." In a sense, our current sample classification is the closest practical approximation to this truth in the absence of historic annual (2000 to 2014) ground surveys or time series of very high resolution data. We therefore can only indirectly assess the possible errors of reference sample classification by analyzing certainty flags for each sampled pixel. A total of 497 sampled pixels (5% of the total sample size of 10,000; 274 "no loss" and 223 "loss") were classified as low-confidence presence/absence of forest loss during sample interpretation (fig. S6). Sample pixels with low-confidence presence/absence of forest loss were spread throughout the region but were somewhat clustered in the cloudy coastal regions, particularly in the DRC province Bas Congo.

Confidence level was recorded separately for each forest loss category (loss year, predisturbance forest type, and loss driver), for both high- and low-confidence sample pixels identified as loss. Years with the highest percentage of forest loss area coming from low-confidence sample pixels (potential commission error) were 2007 (34%), 2003 (25%), and 2002 (25%); years with the lowest percentage were 2011 (9%), 2006 (10%), and 2010 (10%). Annual estimates for 2008 to 2014 had, on average, a smaller proportion of area coming from low-confidence sampled pixels compared with 2001 to 2007 (14% versus 20%), which may be related to a better availability of cloud-free Landsat data (fig. S5) and the very high resolution imagery from Google Earth in the later years. For the forest disturbance drivers, percentage of area coming from low-confidence sampled pixels was the highest in the two smallest classes: mining (55%) and natural disturbances (48%), followed by semipermanent small-scale clearing for agriculture (24%), logging (14%), large-scale clearing for agriculture (14%), fires (8%), rotational small-scale clearing for agriculture (5%), road construction (4%), and commercial and residential construction (2%). These differences could be related to the higher ambiguity of definitions for some of the classes. For example, construction classes are the least ambiguous, since they usually occur in the vicinity with already built-up areas and have a distinct postdisturbance spectral signature (concrete and dirt). Mining also has a distinct postdisturbance bare ground signature, but artisanal mining typical for the region is likely to be confused with natural disturbances (e.g., river meandering). Among the predisturbance forest categories, young secondary HTFs, secondary woodlands, and plantations had the highest potential commission error (22, 15, and 22%, respectively), due to their likely confusion with non-woody vegetation (young fallows, tall crops, and shrub). Primary and mature secondary HTFs and primary woodlands and dry forests had lower potential commission error rates (7 and 6%).

SUPPLEMENTARY MATERIALS

Supplementary material for this article is available at http://advances.sciencemag.org/cgi/content/full/4/11/eaat2993/DC1

REFERENCES AND NOTES

1. A. Chhatre, A. Agrawal, Trade-offs and synergies between carbon storage and livelihood benefits from forest commons. Proc. Natl. Acad. Sci. U.S.A. 106, 17667–17670 (2009).
2. Y. T. Tegegne, M. Lindner, K. Fobissie, M. Kanninen, Evolution of drivers of deforestation and forest degradation in the Congo Basin forests: Exploring possible policy options to address forest loss. Land Use Policy 51, 312–324 (2016).
3. T. K. Rudel, The national determinants of deforestation in sub-Saharan Africa. Philos. Trans. R. Soc. Lond. B Biol. Sci. 368, 20120405 (2013).
4. Q. Zhang, D. Devers, A. Desch, C. O. Justice, J. Townshend, Mapping tropical deforestation in Central Africa. Environ. Monit. Assess. 101, 69–83 (2005).
5. C. Megevand, A. Mosnier, J. Hourticq, K. Sanders, N. Doetinchem, C. Streck, Deforestation Trends in the Congo Basin: Reconciling Economic Growth and Forest Protection (The World Bank, 2013).
6. F. Grigoli, A. Herman, A. Swiston, "A Crude Shock: Explaining the Impact of the 2014-16 Oil Price Decline Across Exporters," IMF Working Paper 17/160, International Monetary Fund, 2017.
7. P. Mayaux, J.-F. Pekel, B. Desclée, F. Donnay, A. Lupi, F. Achard, M. Clerici, C. Bodart, A. Brink, R. Nasi, A. Belward, State and evolution of the African rainforests between 1990 and 2010. Philos. Trans. R. Soc. Lond. B Biol. Sci. 368, 20120300 (2013).
8. B. Fisher, African exception to drivers of deforestation. Nat. Geosci. 3, 375–376 (2010).
9. S. Wunder, Oil Wealth and the Fate of the Forest: A Comparative Study of Eight Countries, Routledge Explorations in Environmental Economics (Routledge Press, 2005).
10. N. T. Laporte, J. A. Stabach, R. Grosch, T. S. Lin, S. J. Goetz, Expansion of industrial logging in Central Africa. Science 316, 1451 (2007).
11. L. Feintrenie, Agro-industrial plantations in Central Africa, risks and opportunities. Biodivers. Conserv. 23, 1577–1589 (2014).
12. TFA, "Tropical Forest Alliance 2020 Marrakesh Declaration for Sustainable Development of the Oil Palm Sector in Africa, UNFCCC Twenty-Second Session of the Conference of the Parties" (2012).
13. Government of Gabon, "Strategic Plan for an Emerging Gabon. Plan Strategique Gabon Emergent: Vision 2025 et orientations stratégiques 2011-2016" (2012).
14. M. C. Hansen, P. V. Potapov, R. Moore, M. Hancher, S. A. Turubanova, A. Tyukavina, D. Thau, S. V. Stehman, S. J. Goetz, T. R. Loveland, A. Kommareddy, A. Egorov, L. Chini, C. O. Justice, J. R. G. Townshend, High-resolution global maps of 21st-century forest cover change. Science 342, 850–853 (2013).
15. D. H. Kim, J. O. Sexton, P. Noojipady, C. Huang, A. Anand, S. Channan, M. Feng, J. R. Townshend, Global, Landsat-based forest-cover change from 1990 to 2000. Remote Sens. Environ. 155, 178–193 (2014).
16. P. V. Potapov, S. A. Turubanova, M. C. Hansen, B. Adusei, M. Broich, A. Altstatt, L. Mane, C. O. Justice, Quantifying forest cover loss in Democratic Republic of the Congo, 2000–2010, with Landsat ETM + data. Remote Sens. Environ. 122, 106–116 (2012).
17. A. Tyukavina, A. Baccini, M. C. Hansen, P. V. Potapov, S. V. Stehman, R. A. Houghton, A. M. Krylov, S. Turubanova, S. J. Goetz, Aboveground carbon loss in natural and managed tropical forests from 2000 to 2012. Environ. Res. Lett. 10, 074002 (2015).
18. F. Achard, R. Beuchle, P. Mayaux, H. J. Stibig, C. Bodart, A. Brink, S. Carboni, B. Desclée, F. Donnay, H. D. Eva, A. Lupi, R. Rāši, R. Seliger, D. Simonetti, Determination of tropical deforestation rates and related carbon losses from 1990 to 2010. Glob. Chang. Biol. 20, 2540–2554 (2014).
19. P. Olofsson, G. M. Foody, M. Herold, S. V. Stehman, C. E. Woodcock, M. A. Wuldere, Good practices for estimating area and assessing accuracy of land change. Remote Sens. Environ. 148, 42–57 (2014).
20. GFOI, Integration of Remote-Sensing and Ground-Based Observations for Estimation of Emissions and Removals of Greenhouse Gases in Forests: Methods and Guidance from

the Global Forest Observations Initiative. Edition 2.0 (Food and Agriculture Organization, 2016).

21. N. Hosonuma, M. Herold, V. De Sy, R. S. De Fries, M. Brockhaus, L. Verchot, A. Angelsen, E. Romijn, An assessment of deforestation and forest degradation drivers in developing countries. *Environ. Res. Lett.* **7**, 044009 (2012).

22. R. A. Houghton, Carbon emissions and the drivers of deforestation and forest degradation in the tropics. *Curr. Opin. Environ. Sustain.* **4**, 597–603 (2012).

23. C. Ernst, P. Mayaux, A. Verhegghen, C. Bodart, M. Christophe, P. Defourny, National forest cover change in Congo Basin: Deforestation, reforestation, degradation and regeneration for the years 1990, 2000 and 2005. *Glob. Chang. Biol.* **19**, 1173–1187 (2013).

24. A. Tyukavina, M. C. Hansen, P. V. Potapov, S. V. Stehman, K. Smith-Rodriguez, C. Okpa, R. Aguilar, Types and rates of forest disturbance in Brazilian Legal Amazon, 2000–2013. *Sci. Adv.* **3**, e1601047 (2017).

25. A. Tyukavina, S. V. Stehman, P. V. Potapov, S. A. Turubanova, A. Baccini, S. J. Goetz, N. T. Laporte, R. A. Houghton, M. C. Hansen, National-scale estimation of gross forest aboveground carbon loss: A case study of the Democratic Republic of the Congo. *Environ. Res. Lett.* **8**, 044039 (2013).

26. R. Tropek, O. Sedláček, J. Beck, P. Keil, Z. Musilová, I. Šímová, D. Storch, Comment on "High-resolution global maps of 21st-century forest cover change." *Science* **344**, 981 (2014).

27. P. C. J. Moonen, B. Verbist, J. Schaepherders, M. B. Meyi, A. Van Rompaey, B. Muys, Actor-based identification of deforestation drivers paves the road to effective REDD+ in DR Congo. *Land Use Policy* **58**, 123–132 (2016).

28. F. Zvomuya, On a whim: Equatorial Guinea building new capital city in the middle of the rainforest. *Mongabay Environ. News* (2014).

29. G. Molinario, M. C. Hansen, P. V. Potapov, Forest cover dynamics of shifting cultivation in the Democratic Republic of Congo: A remote sensing- based assessment for 2000 – 2010. *Environ. Res. Lett.* **10** (2015).

30. J. A. Sayer, D. Endamana, M. Ruiz-Perez, A. K. Boedhihartono, Z. Nzooh, A. Eyebe, A. Awono, L. Usongo, Global financial crisis impacts forest conservation in Cameroon. *Int. For. Rev.* **14**, 90–98 (2012).

31. D. Nepstad, D. McGrath, C. Stickler, A. Alencar, A. Azevedo, B. Swette, T. Bezerra, M. DiGiano, J. Shimada, R. Seroa da Motta, E. Armijo, L. Castello, P. Brando, M. C. Hansen, M. McGrath-Horn, O. Carvalho, L. Hess, Slowing Amazon deforestation through public policy and interventions in beef and soy supply chains. *Science* **344**, 1118–1123 (2014).

32. S. A. Abood, J. S. H. Lee, Z. Burivalova, J. Garcia-Ulloa, L. P. Koh, Relative contributions of the logging, fiber, oil palm, and mining industries to forest loss in Indonesia. *Conserv. Lett.* **8**, 58–67 (2015).

33. S. Turubanova, P. V. Potapov, A. Tyukavina, M. C. Hansen, Ongoing primary forest loss in Brazil, Democratic Republic of the Congo, and Indonesia. *Environ. Res. Lett.* **13**, 074028 (2018).

34. P. S. Dasgupta, Population, poverty and the local environment. *Sci. Am.* **272**, 40–45 (1995).

35. E. Boserup, *Population and Technological Change: A Study of Long-Term Trends* (The University of Chicago Press, 1965).

36. D. L. Carr, Proximate population factors and deforestation in tropical agricultural frontiers. *Popul. Environ.* **25**, 585–612 (2004).

37. K. Vlassenroot, T. Raeymaekers, *Conflict and Social Transformation in Eastern DR Congo* (Academia Press, 2004).

38. FAO, *Living in and from the Forests of Central Africa* (Rome, 2017).

39. P. Potapov, M. C. Hansen, L. Laestadius, S. Turubanova, A. Yaroshenko, C. Thies, W. Smith, I. Zhuravleva, A. Komarova, S. Minnemeyer, E. Esipova, The last frontiers of wilderness: Tracking loss of intact forest landscapes from 2000 to 2013. *Sci. Adv.* **3**, e1600821 (2017).

40. V. Foster, W. Butterfield, C. Chen, N. Pushak, "Building Bridges: China's Growing Role as Infrastructure Financier for Sub-Saharan Africa. Trends and Policy Options; no. 5" (The World Bank, 2009).

41. FAO, *Global Forest Resources Assessment 2015* (2015); http://www.fao.org/forest-resources-assessment/current-assessment/en/.

42. E. N. Chidumayo, D. J. Gumbo, The environmental impacts of charcoal production in tropical ecosystems of the world: A synthesis. *Energy Sustain. Dev.* **17**, 86–94 (2013).

43. G. Molinario, M. C. Hansen, P. V. Potapov, A. Tyukavina, S. Stehman, B. Barker, M. Humber, Quantification of land cover and land use within the rural complex of the Democratic Republic of Congo. *Environ. Res. Lett.* **12**, 104001 (2017).

44. A. Tyukavina, M. C. Hansen, P. V. Potapov, A. M. Krylov, S. J. Goetz, Pan-tropical hinterland forests: Mapping minimally disturbed forests. *Glob. Ecol. Biogeogr.* **25**, 151–163 (2016).

45. D. Butler, Many eyes on Earth: Swarms of small satellites set to deliver close to real-time imagery of swathes of the planet. *Nature* **505**, 143–144 (2014).

46. M. Hirschmugl, M. Steinegger, H. Gallaun, M. Schardt, Mapping forest degradation due to selective logging by means of time series analysis: Case studies in Central Africa. *Remote Sens.* **6**, 756–775 (2014).

47. B. Pengra, J. Long, D. Dahal, S. V. Stehman, T. R. Loveland, A global reference database from very high resolution commercial satellite data and methodology for application to Landsat derived 30m continuous field tree cover data. *Remote Sens. Environ.* **165**, 234–248 (2015).

48. J.-F. Bastin, N. Berrahmouni, A. Grainger, D. Maniatis, D. Mollicone, R. Moore, C. Patriarca, N. Picard, B. Sparrow, E. M. Abraham, K. Aloui, A. Atesoglu, F. Attore, Ç. Bassüllü, A. Bey, M. Garzuglia, L. G. García-Montero, N. Groot, G. Guerin, L. Laestadius, A. J. Lowe, B. Mamane, G. Marchi, P. Patterson, M. Rezende, S. Ricci, I. Salcedo, A. Sanchez-Paus Diaz, F. Stolle, V. Surappaeva, R. Castro, The extent of forest in dryland biomes. *Science* **358**, 635–638 (2017).

49. M. Broich, S. V. Stehman, M. C. Hansen, P. Potapov, Y. E. Shimabukuro, A comparison of sampling designs for estimating deforestation from Landsat imagery: A case study of the Brazilian Legal Amazon. *Remote Sens. Environ.* **113**, 2448–2454 (2009).

50. Q. Ying, M. C. Hansen, P. V. Potapov, A. Tyukavina, L. Wang, S. V. Stehman, R. Moore, M. Hancher, Global bare ground gain from 2000 to 2012 using Landsat imagery. *Remote Sens. Environ.* **194**, 161–176 (2017).

51. A. Bey, A. Sánchez-Paus Díaz, D. Maniatis, G. Marchi, D. Mollicone, S. Ricci, J.-F. Bastin, R. Moore, S. Federici, M. Rezende, C. Patriarca, R. Turia, G. Gamoga, H. Abe, E. Kaidong, G. Miceli, Collect earth: Land use and land cover assessment through augmented visual interpretation. *Remote Sens.* **8**, 807 (2016).

52. IPCC, *2006 IPCC Guidelines for National Greenhouse Gas Inventories. Volume 1: General Guidance and Reporting* (IGES, 2006).

53. M. C. Hansen, P. V. Potapov, S. J. Goetz, S. Turubanova, A. Tyukavina, A. Krylov, A. Kommareddy, A. Egorov, Mapping tree height distributions in Sub-Saharan Africa using Landsat 7 and 8 data. *Remote Sens. Environ.* **185**, 221–232 (2016).

54. T. Mitche, J. K. Zimmerman, J. B. Pascarella, L. Rivera, H. Marcano-Vega, Forest regeneration in a chronosequence of tropical abandoned pastures: Implications for restoration ecology. *Restor. Ecol.* **8**, 328–338 (2000).

55. S. V. Stehman, Sampling designs for accuracy assessment of land cover. *Int. J. Remote Sens.* **30**, 5243–5272 (2009).

56. S. V. Stehman, Estimating area and map accuracy for stratified random sampling when the strata are different from the map classes. *Int. J. Remote Sens.* **35**, 4923–4939 (2014).

57. W. G. Cochran, *Sampling Techniques* (John Wiley & Sons Inc., ed. 3, 1977).

58. P. V. Potapov, S. A. Turubanova, A. Tyukavina, A. M. Krylov, J. L. McCarty, V. C. Radeloff, M. C. Hansen, Eastern Europe's forest cover dynamics from 1985 to 2012 quantified from the full Landsat archive. *Remote Sens. Environ.* **159**, 28–43 (2015).

Citation: A. Tyukavina, M. C. Hansen, P. Potapov, D. Parker, C. Okpa, S. V. Stehman, I. Kommareddy, S. Turubanova, Congo Basin forest loss dominated by increasing smallholder clearing. *Sci. Adv.* **4**, eaat2993 (2018).

Science Advances

Congo Basin forest loss dominated by increasing smallholder clearing

Alexandra Tyukavina, Matthew C. Hansen, Peter Potapov, Diana Parker, Chima Okpa, Stephen V. Stehman, Indrani Kommareddy and Svetlana Turubanova

ARTICLE TOOLS	http://advances.sciencemag.org/content/4/11/eaat2993
SUPPLEMENTARY MATERIALS	http://advances.sciencemag.org/content/suppl/2018/11/05/4.11.eaat2993.DC1
REFERENCES	This article cites 43 articles, 7 of which you can access for free http://advances.sciencemag.org/content/4/11/eaat2993#BIBL
PERMISSIONS	http://www.sciencemag.org/help/reprints-and-permissions

Use of this article is subject to the Terms of Service